Check for updates

Article

Human and Experimental Toxicology
2021, Vol. 40(1) 136–147
© The Author(s) 2020
Article reuse guidelines:
sagepub.com/journals-permissions
DOI: 10.1177/0960327120946470
journals.sagepub.com/home/het
SAGE

Hepatic injury induced by radio frequency waves emitted from conventional Wi-Fi devices in Wistar rats

HM Fahmy[1] and FF Mohammed[2]

Abstract

In this study, the impact of standard 2.45 GHz radio frequency source (averaged whole-body specific absorption rate 0.01 W kg^{-1} 24 h^{-1} daily for 40 consecutive days) on the liver of Wistar female rats was investigated. The rats were randomly divided into control and Wi-Fi–exposed groups. At the end of the exposure, liver samples were dissected from rats. Rats' livers were inspected through the evaluation of some oxidative stress parameters and the evaluation of glutamic oxaloacetic transaminase and glutamic-pyruvic transaminase levels as well as through the molecular investigation using Fourier transform infrared spectroscopy. Histopathological examination in addition to ultrastructure examination was also performed. The present data revealed that Wi-Fi exposure leads to severe oxidative stress in the rat liver. Furthermore, Wi-Fi exposure resulted in deleterious effects in the liver function and alters its molecular structure. Moreover, severe histological and ultrastructural alterations are reported in the hepatic tissues points to hepatotoxic effects induced by Wi-Fi exposure. In conclusion, care must be taken when using Wi-Fi emitting devices due to their severe impact on the liver. Public awareness of the need to decrease exposure time and increase the distance from Wi-Fi exposure sources must be raised wherever possible.

Keywords

Liver, electromagnetic radiation, oxidative stress, apoptosis, ultrastructure, Wi-Fi, FTIR

Introduction

Wireless local area network systems (2.45 GHz) showed a widespread nowadays and widely replaced wired internet access, and they are being applied in universities, schools, households, and public areas.[1,2] During the last decade, the biological impacts of electromagnetic radiation (EMR) and their possible effects attracted great interest and have been the scope of several studies; nonetheless, the output of these studies is still scarce and conflicting.

Reactive oxygen substances (ROS) are the yield of many biological processes, such as phagocyte activity and mitochondrial functions. ROS result in severe oxidative injury in several biomolecules, such as proteins, lipids, and nucleic acids.[3,4] Previous studies indicated that the main site for EMR detoxification is the human liver and that EMR may induce hepatotoxicity.[5,6]

In a previous study of Çetin et al.,[7] the authors revealed that new-born rats (4–6 weeks) irradiated with 2.45-GHZ EMR recorded changes in the oxidative stress status in both brain and liver. Whether EMR can cause deleterious adverse effects on the liver oxidative stress or not is still a conflicting issue.[7–13] Salah et al.[14] demonstrated that the exposure of rats to EMR (2.45 GHz, 1 h day^{-1} during 21 consecutive days) increased malondialdehyde (MDA) concentration in liver and kidneys.

The present work aims to evaluate the possible deleterious effects of radio frequency (RF) radiation (2.45 GHz, 24 h day^{-1} for 40 consecutive days)

[1]Biophysics Department, Faculty of Science, Cairo University, Giza, Egypt
[2]Pathology Department, Faculty of Veterinary Medicine, Cairo University, Giza, Egypt

Corresponding author:
HM Fahmy, Biophysics Department, Faculty of Science, Cairo University, 16 Alzafer Street, Haram, Giza 11111, Egypt.
Email: hfahmy@sci.cu.edu.eg

emitted from indoor Wi-Fi Internet access devices using 802.11.b wireless standards on the liver antioxidant redox system in addition to histopathology, the ultrastructure, and some functional tests in the liver of female Wistar rats.

Materials and methods

Animals

Female Wistar rats were used in the present work (average weight 101 $\pm$ 3.00, age 40 days at the start of the experiment), and they were received from a local provider. The animals were kept under fixed appropriate conditions of housing. The water and chow were provided ad libitum. All animals received humane care in accordance with the guidelines of the Institutional Animal Care and Use Committee (IACUC), Faculty of Science, Cairo University (IACUC approval number: CUFSF Biophy 42 14).

Chemicals

Phosphate buffer pH 7.4 (50 mM L^{-1}, Triton X-100 (1%), ethylenediaminetetraacetic acid 0.5 mM) and kits for evaluating oxidative stress parameters were acquired from Bio diagnostic Co., Giza, Egypt. Kits used for measuring glutamic oxaloacetic transaminase (GOT) and glutamic-pyruvic transaminase (GPT) levels were purchased from Diamond Co. (Cairo, Egypt).

Experimental design and exposure system

An indoor wireless access point (2.450 GHz) was used as the RF wave emitter. Rats belonging to each group were divided into two cages, six rats per cage. For the Wi-Fi–irradiated group, the access point from the Wi-Fi device (with 802.11.b mode and WPA2 network protection) integrated two omnidirectional antennas that were set up for internet broadcast via wireless at 2.45 GHz. The used access point was midway positioned between the two cages with a separation distance of 25 cm between each cage and the access point, as viewed in Figure 1. The special distribution of the EMR power density was measured with a field meter (Narda, EMR200, frequency from 0 GHz to 4 GHz, Germany). The averaged whole-body specific absorption rate was 0.01 W kg^{-1}, and it was calculated through the finite-difference time-domain method using the XFDTD Bio-pro software (version: 6.3.8.4, New York, USA). It should be noted here that no temperature rise was detected along the whole experiment. Rats were exposed to RF radiation with the same power density as that measured by the field meter through the experimental procedure process.



Figure 1. Exposure system design (a standard 2.45-GHz radio frequency source with 802.11.b mode and WPA2 network protection).

Control rats were positioned 15 m away from the Wi-Fi source, completely deprived from any RF exposure in the same testing room to affront the same conditions as the exposed group.

Twenty-four female Wistar rats were classified randomly into experimental (Wi-Fi–irradiated group) and control groups, each group comprises 12 rats. Rats were housed in groups of six per cage at 25°C under a 12-h:12-h light/dark cycle. Rats were left 1 week in their cage before the start of the experiment for lab acclimatization. The Wi-Fi–irradiated group was exposed to RF radiation (2.450 GHz) for 24 h day^{-1} for 40 successive days. The control group rats affronted the same conditions as the irradiated rats except for radiation exposure. The weight of all rats was scored at the start and on the day before decapitation. At the end of the experimental period, blood samples were collected, and the serum was separated. Retro-orbital bleeding was the method used to collect blood from animals, a capillary tube was used to disrupt the retrobulbar venous sinus located behind the eye. After that, rats were euthanized by sudden decapitation. The livers were dissected, cleaned of fat, weighed, and kept on −80°C until usage. Among the 12 rats in each group, six rats were used for the determination of oxidative stress parameters and the other six rats for histopathological, ultrastructure examinations besides Fourier transform infrared spectroscopy.

Histopathological examination

After decapitation, rats' livers were fixed in buffered neutral 10% formalin, embedded in paraffin, and sectioned at 8 μm thickness. This was followed by staining the liver sections with hematoxylin and eosin (H&E) according to the method of Banchroft et al.[15]

Slides were then examined with the aid of a light microscope (Zeiss, Germany) to investigate any histopathological lesions in rat livers.

Ultrastructure examination

Five to ten small pieces of 1×1 mm^2 size were separated from livers and then fixed immediately in 5% cold glutaraldehyde. After that, the specimens were washed in cacodylate buffer (pH 7.2) three to four times, each for 20 min and then, postfixed at 1% O_4S_4 for 2 h. After that, the specimens were washed four times in the same buffer, dehydration was done by grading in ascending grades of alcohol (30-50-70-90 and 100%). Then, the specimens were embedded in epon–araldite mixture according to Bozzola and Russell.[16] Next to that, semithin sectioning of embedded block was performed by LKB microtome at 0.5 μm for orientation of tissues and photographed by Sc 30 Olympus camera. Ultrathin sectioning of tissues at 500–700 A was done using Leica AG ultramicrotome and contrasted with uranyl acetate and lead citrate and examined by TEM 100 CXII electron microscope (Olympus) at 780 kV and then photographed by CCD digital camera model XR-41 (IMPERX).

Biochemical analysis

Tissue homogenization. In a motor-driven tissue homogenizer with the aid of phosphate buffer (pH 7.4), liver tissues were homogenized. Unbroken cells, cell debris, and nuclei were centrifuged at $7012 \times g$ for 15 min, and the supernatant was pipetted into plastic tubes and stored at -80°C until assayed.

Determination of lipid peroxidation. Lipid peroxidation was estimated through the measurement of the levels of MDA in the liver tissues. MDA was evaluated by measuring thiobarbituric reactive species following the method of Ruiz-Larrea et al.,[17] in which the pinkish-colored chromogen formed due to the reaction of thiobarbituric acid with lipid peroxidation breakdown products was measured spectrophotometrically at 532 nm in Thermo Spectronic Helios Alpha (UVA 111615, England).

Determination of reduced glutathione levels. The determination of reduced glutathione (GSH) levels was performed using Biodiagnostic kit no. GR 25 11, which is mainly based on the spectrophotometric method of Beutler.[18] It essentially relies on the reduction of 5,5′-dithiobis-2-nitrobenzoic acid with GSH to produce a yellowish color of which the absorbance is measured at 405 nm in a Thermo Spectronic Helios Alpha (UVA 111615).

Determination of catalase activity. Catalase (CAT) activity was evaluated using Biodiagnostic kit no. CA 25 17, which is based on the spectrophotometric method described by Aebi.[19] Briefly, the CAT reacts with a known quantity of hydrogen peroxide and the reaction is stopped after 1 min with CAT inhibitor. In the presence of peroxidase, the remaining hydrogen peroxide reacts with 3,5-dichloro-2-hydroxybenzene sulfonic acid and 4-aminophenazone to yield a chromophore having a color intensity inversely proportional to the activity of CAT in the sample. The absorbance of chromophore color is read at 510 nm in a Thermo Spectronic Helios Alpha (UVA 111615, England).

Determination of glutathione-S-transferase activity. Glutatione-*S*-transferase (GST) activity was assayed following the method of Habig et al.[20] Briefly, 0.4 mL potassium phosphate buffer (50 mmol L^{-1}; pH 6.5), 0.1 mL of supernatant, 1.2 mL water, and 0.1 mL 1-chloro-2, 4 dinitrobenzene, 30 mmol L^{-1} were added and then incubated in a water bath at 37°C for 10 min. After incubation, 0.1 mL of reduced GSH (30 mmol L^{-1}) was added. At 1-min interval, the change in absorbance was measured at 340 nm.

Determination of superoxide dismutase activity. Superoxide dismutase (SOD) activity was determined according to the method of Nishikimi et al.[21] The assay for SOD levels was performed using Biodiagnostic kit no. SD 25 21. This assay relies on the capability of the enzyme to inhibit the phenazine methosulphate-mediated reduction of nitroblue tetrazolium dye.

Determination of nitric oxide levels. The determination of nitric oxide (NO) levels was carried out using Biodiagnostic kit no. NO 25 33. This method is based on the spectrophotometric method of Montgomery and Dymock,[22] which depends on the evaluation of endogenous nitrite concentration as an indicator of NO production. The resulting azo dye has a bright reddish-purple color, whose absorbance is read at 540 nm in a Thermo Spectronic Helios Alpha (UVA 111615).

Determination of serum GOT and serum GPT levels

The levels of GOT and GPT were determined in the blood serum based on the method of Kaneko et al.[23]

Table 1. Effect of Wi-Fi exposure ($F = 2450$ MHz, 24 h daily for 40 days) on some oxidative and antioxidative stress parameters in the livers of female Wistar rats.[a]

Oxidative stress parameters	Control group	Wi-Fi–irradiated group	Percentage difference (%D)	Independent sample *t*-test (*p* value)
MDA (nmol g^{-1} tissue)	2.05 ± 0.27 (6)	6.32 ± 0.87 (6)	208.29%	8.55×10^{-4}[(b)]
GSH (mg g^{-1} tissue)	8.74 ± 0.88 (6)	4.58 ± 0.15 (6)	−47.63%	9.20×10^{-4}[(b)]
Catalase (U g^{-1})	0.91 ± 0.05 (6)	0.77 ± 0.07 (6)	−15.38%	0.14 (n.s.)
GST (U g^{-1} tissue)	4.48 ± 0.25 (6)	3.27 ± 0.62 (6)	−27.01%	0.103 (n.s.)
SOD (U g^{-1} tissue)	463.52 ± 30.07 (6)	305.32 ± 23.76 (6)	−34.13%	0.002[(b)]
NO (μmol g^{-1})	1.44 ± 0.11 (6)	1.31 ± 0.10 (6)	−9.03%	0.40 (n.s.)

% D: percentage difference in comparison to control group; SEM: standard error of the mean; n.s.: nonsignificant.
[a]The number of animals is shown between parentheses. Values represent the mean ± SEM.
[b]$p < 0.05$ significant.

Fourier transform infrared spectroscopy of liver tissues

The liver samples were grained with potassium bromide grade in the ratio of 1:100 and compressed using a hydraulic press under a pressure of 15,000 lbs. The pellets were then scanned in an inert atmosphere over a wavenumber range of 4000–400 cm^{-1} in Hitachi 295 spectrophotometer (Jasco, Mod 4100, Japan).

Statistical analysis

Data of GPT and GOT levels, and oxidative stress parameters were analyzed with the aid of independent sample *t*-test using origin software version 8.0. The percentage difference representing the percent of variation in the value of the treated group with respect to the control was also computed

$$\%\ \text{Difference}\ (\%\ \text{D}) = \left[\begin{array}{l}(\text{treated (radiated) value} - \text{control value})/ \\ (\text{control value})\}\end{array}\right] \times\ 100\%$$

A p value of <0.05 was considered as statistically significant.

Results

Effect of Wi-Fi exposure on some oxidative stress parameters in the liver of female Wistar rats

As depicted from Table 1, in the present study, significant reduction in the activities of antioxidant enzyme SOD besides GSH and NO levels with a concomitant increase in MDA levels was shown in the Wi-Fi–radiated group as compared to the control group.

Effect of Wi-Fi exposure on serum parameters (GOT and GPT levels of female Wistar rats)

As demonstrated in Table 2, the present results showed significant decreases in the GPT levels in the Wi-Fi–exposed group relative to the control group, while GOT recorded nonsignificant changes in both groups.

Effect of Wi-Fi exposure on the Fourier transform infrared spectra of the livers of female Wistar rats

As seen in Figure 2, the position of the absorption peak at 1654 cm^{-1} was largely unchanged, however, it appears weaker in intensity in the Wi-Fi–radiated group relative to the control group. This decline in the 1654 cm^{-1} peak intensity was statistically significant.

Histopathological alterations

The microscopic examination of the control group showed normal histological structure of the liver; there were polyhedral hepatocytes with eosinophilic cytoplasm and basophilic nuclei, and the hepatocytes separated by hepatic sinusoids that were lined by flattened Kupffer cells (Figure 3(a)) and histologically

Table 2. Effect of Wi-Fi exposure on some liver functions in female Wistar rats.[a]

Liver function parameter	Control group	Wi-Fi–radiated group	Percentage difference (%D)	Independent sample *t*-test (*p* value)
GOT	32.69 ± 1.94 (6)	34.79 ± 2.10 (6)	6.42%	0.48 (n.s.)
GPT	16.90 ± 0.76 (6)	14.45 ± 0.77 (6)	−14.50%	0.047[b]

% D: percentage difference in comparison to control group; SEM: standard error of the mean; n.s.: nonsignificant; GOT: glutamic oxaloacetic transaminase; GPT: glutamic-pyruvic transaminase.
[a]Values represent the means ± SEM. The number of animals is shown between parentheses.
[b]$p < 0.05$ significant.

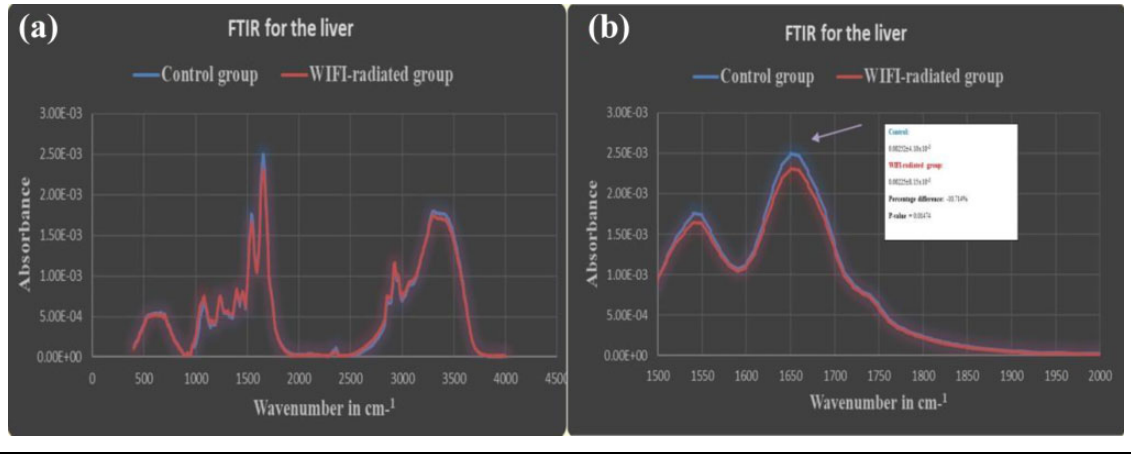


Figure 2. (a) Average FTIR spectra from rat liver tissue. Blue: control group; red: Wi-Fi–radiated group. (b) Zoom of the wavenumber part from 1500 cm^{-1} to 2000 cm^{-1} of the FTIR spectrum. FTIR: Fourier transform infrared.

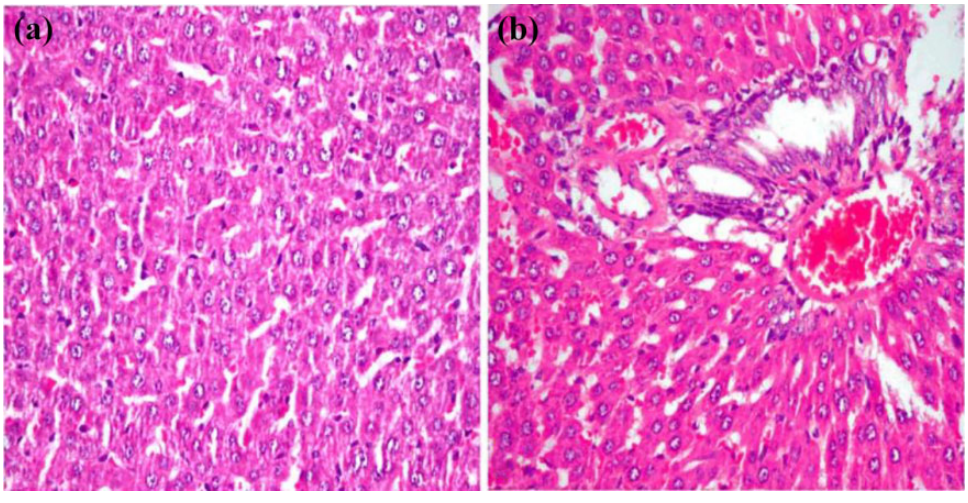


Figure 3. Histological liver section from control group showing (a) normal hepatocytes with eosinophilic cytoplasm and centrally located round basophilic nuclei. (b) Portal area containing bile duct, hepatic artery, and portal vein (H&E, ×400). H&E: hematoxylin and eosin.

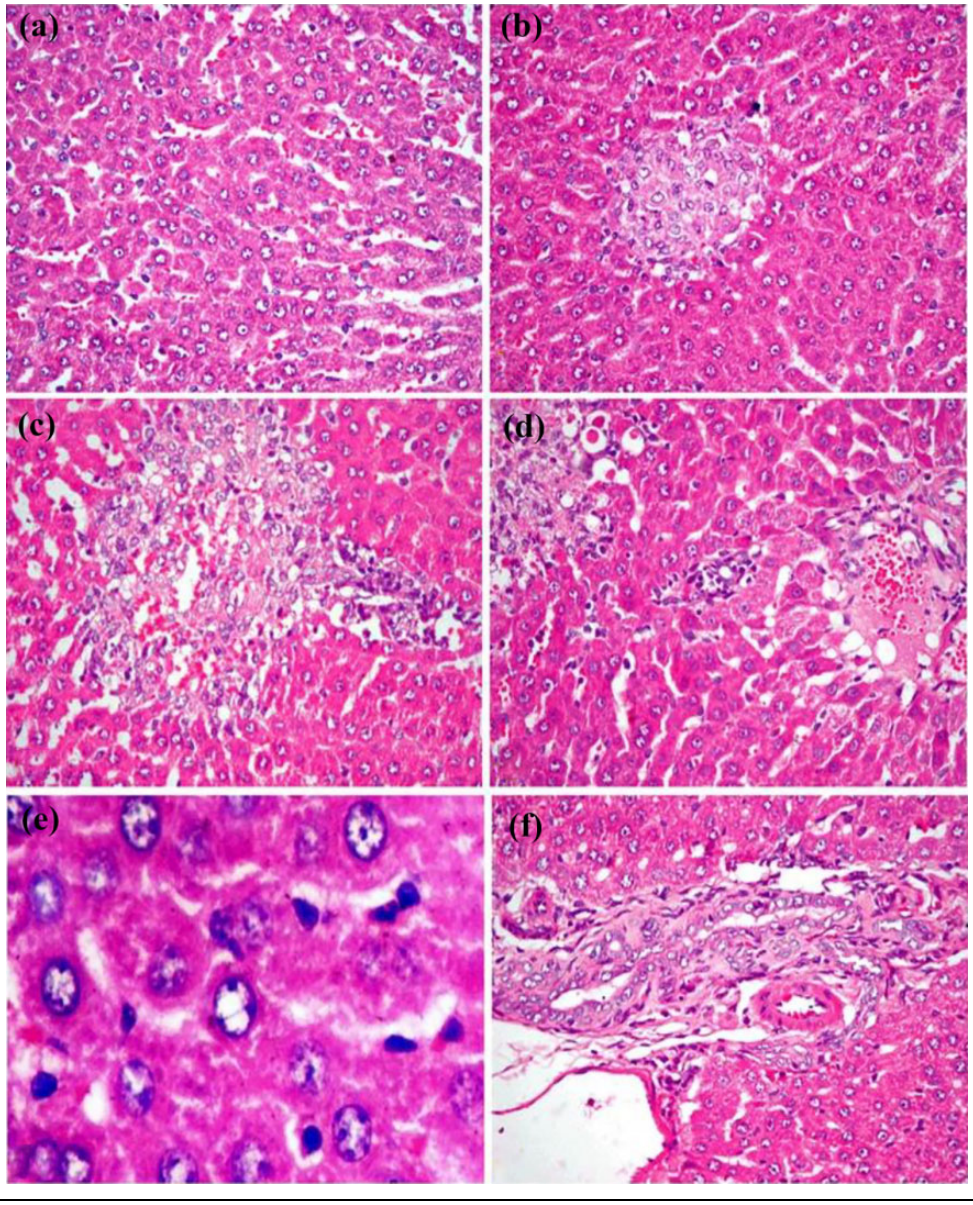


Figure 4. Histological liver section from the irradiated group showing (a–d) H&E, ×400. (a) Binucleated hepatocytes with hypertrophied Kupffer cells. (b) Small foci of hepatocytes showing tinctorial changes with foamy eosinophilic to vaculated cytoplasm with anisokaryosis. (c) Large hepatocellular foci with tinctorial cytoplasmic changes and sinusoidal dilatation and focal mononuclear cell infiltration at the periphery of the lesion. (d) At the left of the image, there are foci of hepatocellular necrosis and apoptosis with the presence of circumscribed eosinophilic apoptotic bodies surrounded by clear hallo associated with small mononuclear cell aggregation. Note the presence of large vacuolated Ito cells in between hepatocytes in parietal area. (e) Hepatocellular nucleus containing intranuclear clear vacuole (H&E, ×1000). (f) Portal area showing hyperplastic bile ductules with mild fibroplasias (H&E, ×400). H&E: hematoxylin and eosin.

normal portal area (Figure 3(b)). The microscopic examination of the liver of the Wi-Fi–radiated group revealed various histopathological alterations. There was a relative increase in binucleated hepatocytes compared with the control group (Figure 4(a)) in addition to the hypertrophy of Kupffer cells lining the sinusoids. There were scattered foci of hepatocytes with altered tinctorial character; these areas ranged from small to large foci and the hepatocellular cytoplasm appeared foamy eosinophilic to clear vacuolated cytoplasm and the nuclei were vesicular and showed anisokaryosis (Figure 4(b) and (c)) with dilated sinusoids. There were foci of necrosis and necroapoptosis; the lesion was characterized by the

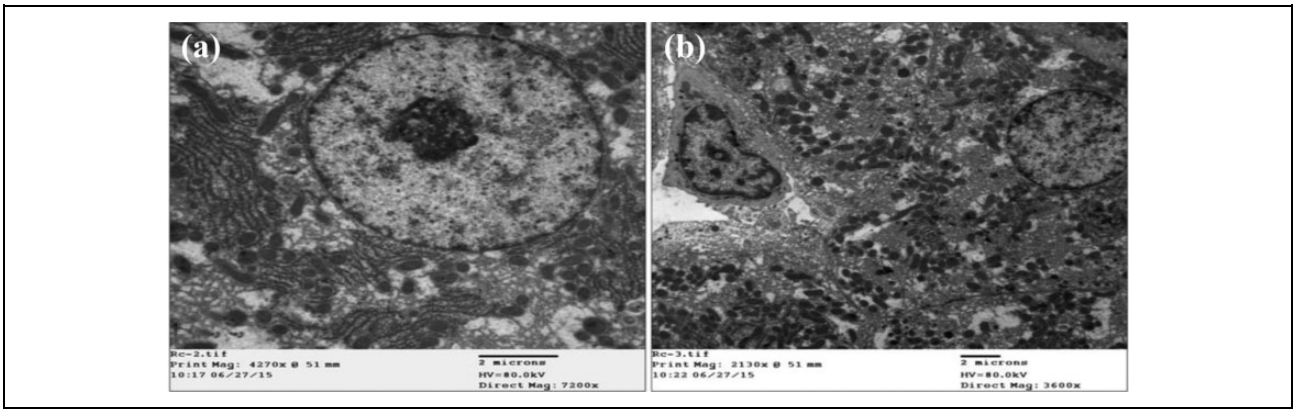


Figure 5. TEM from control rat liver (a) hepatocyte contains large spherical nuclei having mostly one or two nucleoli. The cytoplasm contains rough endoplasmic reticulum, mitochondria, microbodies, small fat globule, and glycogen granules. (b) The hepatic sinusoid containing Kupffer cells having large, prominent nuclei, mitochondria electron dense lysosomes. TEM: transmission electron microscopy.

presence of both necrotic hepatocytes with disintegrated cellular and nuclear structures with mononuclear cell infiltration that were admixed with apoptotic bodies, which are circumscribed round eosinophilic bodies surrounded by clear halo. Ito cells were detected in the periportal area between hepatocytes (Figure 4(d)). Individual vacuolization of hepatocellular nuclei was detected (Figure 4(e)). The portal area showed bile duct hyperplasia with the formation of newly bile ductules associated with oval cell proliferation and mild fibroplasia (Figure 4(f)).

Ultrastructure alterations

The ultrastructure findings of the control group revealed the normal structure of nuclei and cytoplasmic organelles (Figure 5(a)) and normal sized Kupffer cell (Figure 5(b)). However, the ultrastructures of hepatocyte from Wi-Fi–treated group showed the presence of binucleated hepatocyte with dentations of their nuclei and the reduction of the mitochondrial population with the increase of rough endoplasmic reticulum (RER) and microbodies. The hepatocyte showed increased cytoplasmic content of fat and glycogen with the reduction in the cellular cytoplasmic organelles adjacent to mitochondria. In another field, the hepatocyte displays deformed condensed nuclei and disorganized mitochondrial cristae associated with the presence of nonmembranous apoptotic bodies in sinusoidal lumen (Figure 6(a)). On the other hand, necrotic hepatocyte had a small condensed nucleus with few RER and mitochondria with the presence of cytoplasmic fat globule (Figure 6(b)). Necroptosis was identified by the presence of hepatocytes with condensed nucleus, degenerated mitochondrial cristae, and with the presence of the membranous apoptotic body (Figure 6(c)). The hypertrophy of Kupffer cell was identified with increased glycogen content in the adjacent hepatocellular cytoplasm and reduced cell organelles (Figure 6(d)). The space of Disse exhibited the deposition of collagen bundles and hypertrophy of Kupffer cells that contain an enlarged nucleus and numerous vacuoles associated with the presence of lymphocytes (Figure 7(a)). In addition, Ito cell containing fat globules was observed between hepatic cells associated with the presence of collagen bundles (Figure 7(b)). There was a newly formed bile ductule with small lumen; their epithelium had a large nucleus that was rich in free ribosomes besides the reduction in the cell organelles (Figure 7(c)). There was hepatocyte with a dentated condensed nucleus containing nucleolus and fat globule inclusion with increased cytoplasmic fat and glycogen globules content (Figure 7(d)).

Discussion

Uses of Wi-Fi have become growing and are now being involved in many fields of our life; this necessitates the evaluation of the biological impact due to Wi-Fi exposure. The present study aims to investigate the effect of RF waves emitted from conventional Wi-Fi devices on the rat liver. Here, we decided to study the impact of Wi-Fi exposure on the liver because of its importance as it regulates the metabolism of the body and includes important enzymes. The electromagnetic field (EMF) can change the normal cell and tissue life cycle.

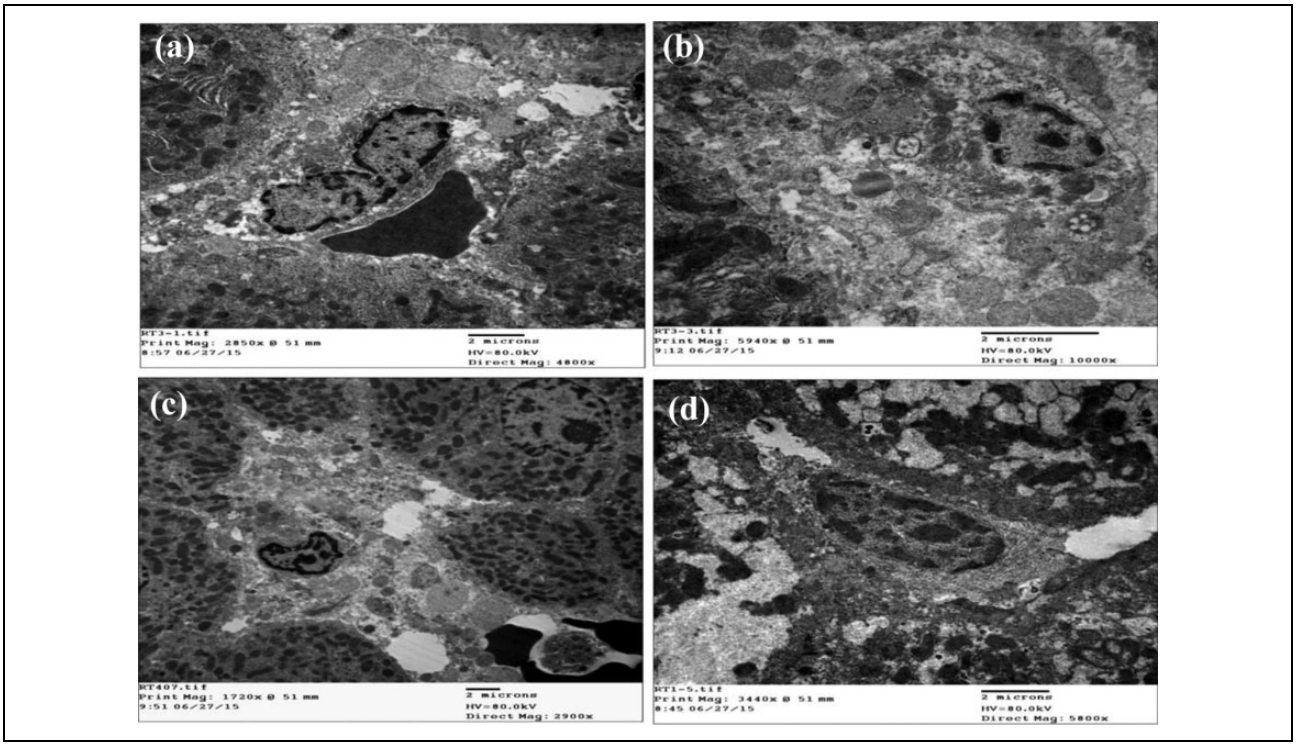


Figure 6. TEM from irradiated rat liver (a) hepatocytes having condensed and folded nucleus with disorganized mitochondrial cristae, numerous fat globules and presence of nonmembranous apoptotic body in sinusoidal lumen. (b) The hepatic sinusoid contains hepatic cells in a state of necrobiosis, where the nucleus becomes small condensed and the cytoplasm reduced, few RER, and numerous electron-lucent mitochondria as well as fat globule. (c) Hepatic sinusoid contains RBCs and small condensed nucleus and remnants of disintegrated hepatocytes and disintegrated mitochondrial cristae and apoptotic bodies. (d) Hepatocytes contain large amounts of glycogen in the cytoplasm with the reduction of the cell organelles and swelling of the cell. The sinusoidal wall lined by hypertrophied Kupffer cell. TEM: transmission electron microscopy; RBC: red blood corpuscle; RER: rough endoplasmic reticulum.

A number of investigations studied the link between the mobile phones operating within frequencies (900–1800 MHz) and oxidative stress, however, there is still a deficiency on the relation between the exposure to 2.45 GHz EMR and oxidative stress.[10,24–28] Even, those studies showed conflicting results.

In the present work, MDA as an oxidative stress marker and antioxidant markers, such as GSH, NO, SOD, CAT, and GST, had been evaluated in rat livers after exposure to Wi-Fi (2.45 GHz, 24 h day^{-1} during 40 consecutive days).

SOD has a very important function in defending the induced oxidative stress, and it catalyzes the conversion of superoxide anions to molecular oxygen and H_2O_2, where the latter can easily diffuse across the biological membranes and can be converted to highly reactive hydroxyl radical.[29–31] Malondialdehyde (MDA) is the product of the oxidation of polyunsaturated fatty acids and it is considered as the main marker for oxidative stress.[32,33] GSH plays important roles as an antioxidant,[34] enzyme cofactor,[35] and cysteine storage form.[36]

We suggest that the significant reduction in GSH and SOD activity could be due to their employment by the enhanced production of ROS and oxidative inactivation of enzyme protein by ROS generation. It has been proven that moderate levels of ROS can cause an increase in antioxidant enzyme activities, whereas very high levels of these reactants were shown to decrease the activities of antioxidant enzymes.[37] The substantial increases in reactive oxygen species (MDA) besides the reduction in the antioxidant defense systems resulting from EMR exposure in the present study may contribute to oxidative stress and consequent liver damage in addition to degradation of liver membranes.

The present work revealed various hepatic histopathological and ultrastructural alterations induced by Wi-Fi exposure, the hepatocytes showed degenerative changes in their cytoplasm with alterations in their tinctorial staining characters, and these changes

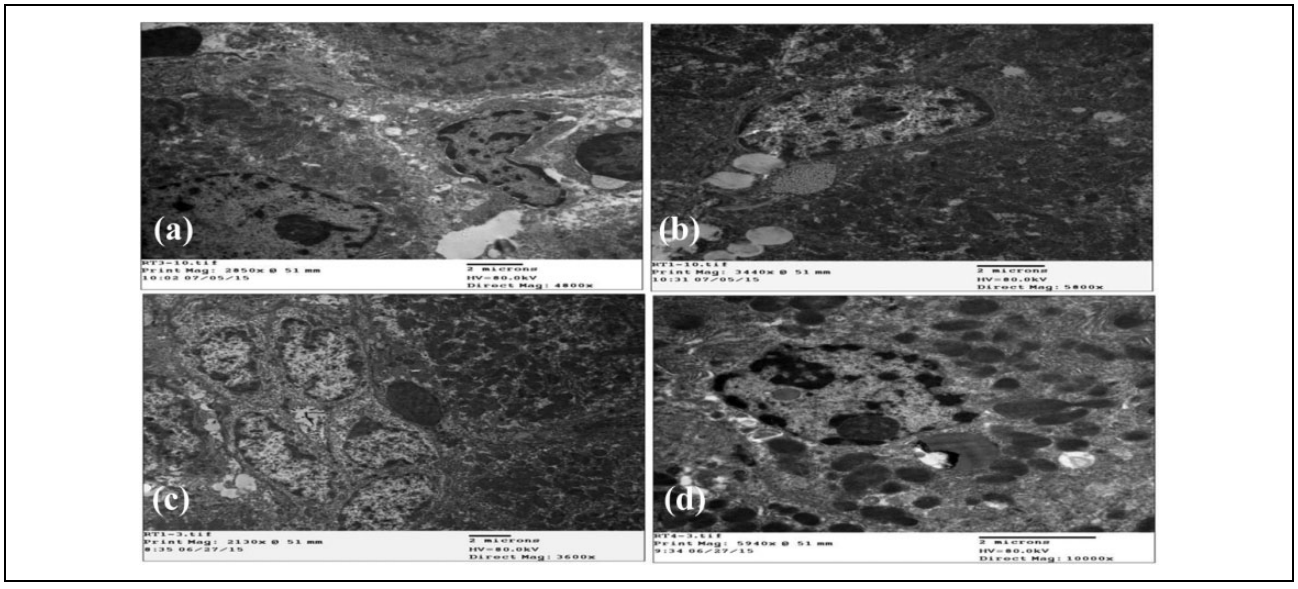


Figure 7. TEM from irradiated rat liver (a) space of Disse showing the presence of bundle of collagen fibers extended between the hepatic cells, hypertrophied Kupffer cell contains numerous vacuoles. (b) Ito cells have fat globule with the presence of collagen fiber extended between the hepatic cells. (c) Hepatic tissue showing the presence of newly formed bile ductules that line of epithelial cell that is rich in free ribosomes and few organelles with reduced ductular lumen size. (d) Hepatocyte nucleus contains a fat globule inclusion and the cytoplasm containing large fat globule and glycogen granules. TEM: transmission electron microscopy.

assumed to be as a result of fat and glycogen accumulation in hepatocellular cytoplasm, resulting in the vacillation of foamy eosinophilic cytoplasm. The histopathology results were further confirmed by the ultrastructural hepatic changes, as there was an accumulation of fat globules as well as glycogen in the cytoplasm of hepatic cells accompanied by a reduction in cellular organelles. The present study proved the damaging effect of EMR on mitochondria resulting in degenerated mitochondrial cristae with subsequent production of ROS.

The elevated ROS level induced by mitochondrial damage results in various histopathological changes, including fatty and glycogen infiltration in hepatocellular cytoplasm, hepatocellular apoptosis, and/or necrosis and Kupffer cell activation, as illustrated by electron microscope and histopathological results. Previous studies revealed the effect of the elevated oxidative stress on hepatocytes. Babu et al.[38] and Mohan et al.[39] found that ROS generation induces ultrastructural changes in hepatocytes and induced apoptosis. In addition, Vollmar and Menger[40] stated that ROS directly control cell apoptosis and necrosis.

Like the results obtained by our study, Çelik et al.[41] investigated the effects of Wi-Fi–induced EMR (2.45 GHz, 1 h day^{-1} for 5 days/week) from pregnancy to 3 weeks of age on the brain and liver antioxidant redox systems in the rat during pregnancy and development. The authors concluded that Wi-Fi–induced oxidative stress in the brain and liver of developing rats. In another study, Salah et al.[14] investigated the effect of olive leaves extract administration on glucose metabolism and oxidative response in liver and kidneys of rats exposed to RF. The authors reported that the exposure of rats to RF (2.45 GHz, 1 h day^{-1} during 21 consecutive days) induced a diabetes-like status. Moreover, RF decreased the activities of GSH peroxidase, CAT, and the SOD, respectively, in liver and kidneys. Indeed, the authors declared that the exposure to RF increased the MDA concentration, respectively, in liver and kidneys. The authors suggested that the RF exposure induced a diabetes-like status through alteration of oxidative response.

The histological and ultrastructure examination revealed a mild increase in the number of Ito cells or hepatic stellate cells (HSCs), which were associated with the proliferation of collagen bundles. Previous research clarified the role of HSCs in the development of liver fibrosis. Canbay et al.[42] clarified that the engulfment of apoptotic hepatocytes by HSC lines induced their activation with subsequent profibrogenic response and also the occurrence of oxidative stress in the hepatic tissue, and activated HSCs and the Kupffer cells.[43,44]

The spectral region 1800–1500 cm^{-1} corresponds primarily to protein absorption bands. The principle protein marker band is the amide I absorption centered around 1654 cm^{-1}. The amide I band position and shape are sensitive to the secondary structures of proteins.[45]

The changes in the amide I band profile reflect significant differences in hydrogen-bonding strengths and differences in transition dipole coupling as these are the factors that give the amide I band its sensitivity to protein secondary conformational changes.[46] A significant reduction in the intensity of the amide I peak is attributed to a loss of secondary amide, which is a proposed mechanism of the deleterious mechanism of damage of liver observed in the present study due to EMR exposure.

Even in scientific communities, potential biological effects on the exposure of EMFs are not yet well established. It is worth to mention that several factors regarding the influence of EMFs on animal models must be investigated before a discussion of possible effects of RF-EMF on the human body.

We recommend the raise of awareness among the public for the necessity of the decrease in the exposure time, increasing the distance from Wi-Fi exposure sources whenever possible.

In conclusion, Wi-Fi exposure in the present study leads to severe oxidative stress in the rat liver besides causing a molecular structural change in the liver protein secondary structure. However, further investigations are still needed to clarify the mechanism of action of the applied EMR exposure and oxidative stress on the rat liver to establish the biological significance of the observed phenomena.

Declaration of conflicting interests

The author(s) declared no potential conflicts of interest with respect to the research, authorship, and/or publication of this article.

Funding

The author(s) received no financial support for the research, authorship, and/or publication of this article.

ORCID iD

HM Fahmy https://orcid.org/0000-0001-8689-1198

References

1. Nazıroğlu M, Yüksel M, Köse SA, et al. Recent reports of Wi-Fi and mobile phone-induced radiation on oxidative stress and reproductive signaling pathways in females and males. *J Membr Biol* 2013; 246(12): 869–875.
2. Dasdag S, Akdag MZ, Erdal ME, et al. Effects of 2.4 GHz radiofrequency radiation emitted from Wi-Fi equipment on microRNA expression in brain tissue. *Int J Radiat Biol* 2015; 91(7): 555–561.
3. Dasdag S, Akdag MZ, Ulukaya E, et al. Effect of mobile phone exposure on apoptotic glial cells and status of oxidative stress in rat brain. *Electr Biol Med* 2009; 28(4): 342–354.
4. Akdag MZ, Dasdag S, Cakir DU, et al. Do 100-and 500-μT ELF magnetic fields alter beta-amyloid protein, protein carbonyl and malondialdehyde in rat brains? *Electr Biol Med* 2013; 32(3): 363–372.
5. De S and Devasagayam TP. Protective effect of an aminothiazole compound against γ-radiation induced oxidative damage. *Free Rad Res* 2011; 45(11–12): 1342–1353.
6. Ferk F, Chakraborty A, Jäger W, et al. Potent protection of gallic acid against DNA oxidation: results of human and animal experiments. *Mutat Res* 2011; 715(1–2): 61–71.
7. Çetin H, Nazıroğlu M, Çelik Ö, et al. Liver antioxidant stores protect the brain from electromagnetic radiation (900 and 1800 MHz)-induced oxidative stress in rats during pregnancy and the development of offspring. *J Matern Fetal Neonatal Med* 2014; 27: 1915–1921.
8. Naziroğlu M and Gümral N. Modulator effects of L-carnitine and selenium on wireless devices (2.45 GHz)-induced oxidative stress and electroencephalography records in brain of rat. *Int J Radiat Biol* 2009; 85(8): 680–689.
9. Takahashi S, Imai N, Nabae K, et al. Lack of adverse effects of whole-body exposure to a mobile telecommunication electromagnetic field on the rat fetus. *Radiat Res* 2010; 173(3): 362–372.
10. Dasdag S, Akdag MZ, Kizil G, et al. Effect of 900 MHz radio frequency radiation on beta amyloid protein, protein carbonyl, and malondialdehyde in the brain. *Electr Biol Med* 2012; 31(1): 67–74.
11. Shahin S, Singh VP, Shukla RK, et al. 2.45 GHz microwave irradiation-induced oxidative stress affects implantation or pregnancy in mice, Mus musculus. *Appl Biochem Biotechnol* 2013; 169: 1727–1751.
12. Ghazizadeh V and Nazıroğlu M. Electromagnetic radiation (Wi-Fi) and epilepsy induce calcium entry and apoptosis through activation of TRPV1 channel in hippocampus and dorsal root ganglion of rats. *Metab Brain Dis* 2014; 29(3): 787–799.
13. Gürler HŞ, Bilgici B, Akar AK, et al. Increased DNA oxidation (8-OHdG) and protein oxidation (AOPP) by

low level electromagnetic field (2.45 GHz) in rat brain and protective effect of garlic. *Int J Radiat Biol* 2014; 90(10): 892–896.
14. Salah MB, Abdelmelek H and Abderraba M. Effects of olive leave extract on metabolic disorders and oxidative stress induced by 2.45 GHz WIFI signals. *Environ Toxicol Pharmacol* 2013; 36(3): 826–834.
15. Banchroft JD, Stevens A and Turner DR. *Theory and practice of histolological techniques*. 4th ed. New York, San Francisco: Churchil Livingstone, 2016.
16. Bozzola J and Russell L. *Electron microscopy: principles and techniques for biologists*, 1991. https://www.abebooks.com/booksearch/title/electronmicroscopy/author/bozzola-j-j/.
17. Ruiz-Larrea MB, Leal AM, Liza M, et al. Antioxidant effects of estradiol and 2-hydroxyestradiol on iron-induced lipid peroxidation of rat liver microsomes. *Steroids* 1994; 59(6): 383–388.
18. Beutler E. Improved method for the determination of blood glutathione. *J Lab Clin Med* 1963; 61: 882–888.
19. Aebi H. 13 Catalase in vitro. In: Abelson J, Simon M, Verdine G, et al. (eds) *Methods in enzymology*. Cambridge: Academic Press, 1984, Vol. 105, pp. 121–126.
20. Habig WH, Pabst MJ and Jakoby WB. Glutathione S-transferases. The first enzymatic step in mercapturic acid formation. *J Biol Chem* 1974; 249: 7130–7139.
21. Nishikimi M, Roa NA and Yogi K. The occurrence of superoxide anion in the reaction of reduced phenazine methosulfate and molecular oxygen. *Biochem Biophys Res Commun* 1972; 46(2): 849–854.
22. Montgomery HA and Dymock JF. Determination of nitrite in water. *Analyst* 1961; 86(102): 414.
23. Kaneko JJ, Harvey JW and Bruss ML. *Clinical biochemistry of domestic animals*. 6th ed. New York: Academic Press, 2008, pp. 881–888.
24. Dasdag S, Akdag MZ, Aksen F, et al. Does 900 MHZ GSM mobile phone exposure affect rat brain? *Electr Biol Med* 2004; 23(3): 201–214.
25. Choi SJ and Choy JH. Layered double hydroxide nanoparticles as target-specific delivery carriers: uptake mechanism and toxicity. *Nanomedicine* 2011; 6(5): 803–814.
26. Avci B, Akar A, Bilgici B, et al. Oxidative stress induced by 1.8 GHz radio frequency electromagnetic radiation and effects of garlic extract in rats. *Int J Radiat Biol* 2012; 88(11): 799–805.
27. Bilgici B, Akar A, Avci B, et al. Effect of 900 MHz radiofrequency radiation on oxidative stress in rat brain and serum. *Electr Biol Med* 2013; 32(1): 20–29.
28. Liu C, Duan W, Xu S, et al. Exposure to 1800 MHz radiofrequency electromagnetic radiation induces oxidative DNA base damage in a mouse spermatocyte-derived cell line. *Toxicol Lett* 2013; 218(1): 2–9.
29. Köylü H, Mollaoglu H, Ozguner F, et al. Melatonin modulates 900 Mhz microwave-induced lipid peroxidation changes in rat brain. *Toxicol Ind Health* 2006; 22(5): 211–216.
30. Kümin A, Huber C, Rülicke T, et al. Peroxiredoxin 6 is a potent cytoprotective enzyme in the epidermis. *Am J Pathol* 2006; 169(4): 1194–1205.
31. Koyu A, Ozguner F, Yilmaz HR, et al. The protective effect of caffeic acid phenethyl ester (CAPE) on oxidative stress in rat liver exposed to the 900 MHz electromagnetic field. *Toxicol Ind Health* 2009; 25(6): 429–434.
32. Ozguner F, Aydin G, Mollaoglu H, et al. Prevention of mobile phone induced skin tissue changes by melatonin in rat: an experimental study. *Toxicol Ind Health* 2004; 20(6–10): 133–139.
33. Ozguner F, Altinbas A, Ozaydin M, et al. Mobile phone-induced myocardial oxidative stress: protection by a novel antioxidant agent caffeic acid phenethyl ester. *Toxicol Ind Health* 2005; 21(7–8): 223–230.
34. Dringen R. Metabolism and functions of glutathione in brain. *Prog Neurobiol* 2000; 62(6): 649–671.
35. Chance B, Sies H and Boveris A. Hydroperoxide metabolism in mammalian organs. *Physiol Rev* 1979; 59(3): 527–605.
36. Generally GS. Multiple roles of glutathione in the central nervous system. *J Biol Chem* 1997; 378: 793–802.
37. Warner J, Epstein M, Sweet A, et al. Genetic testing in familial isolated hyperparathyroidism: unexpected results and their implications. *J Med Genet* 2004; 41(3): 155–160.
38. Babu JR, Sundravel S, Arumugam G, et al. Salubrious effect of vitamin C and vitamin E on tamoxifen-treated women in breast cancer with reference to plasma lipid and lipoprotein levels. *Cancer Lett* 2000; 151(1): 1–5.
39. Mohan M, Taneja TK, Sahdev S, et al. Antioxidants prevent UV-induced apoptosis by inhibiting mitochondrial cytochrome c release and caspase activation in Spodoptera frugiperda (Sf9) cells. *Cell Biol Int* 2003; 27(6): 483–490.
40. Vollmar B and Menger MD. The hepatic microcirculation: mechanistic contributions and therapeutic targets in liver injury and repair. *Physiol Rev* 2009; 89(4): 1269–1339.

41. Çelik Ö, Kahya MC and Nazıroğlu M. Oxidative stress of brain and liver is increased by Wi-Fi (2.45 GHz) exposure of rats during pregnancy and the development of newborns. *J Chem Neuroanat* 2016; 75: 134–139.
42. Canbay A, Taimr P, Torok N, et al. Apoptotic body engulfment by a human stellate cell line is profibrogenic. *Lab Invest* 2003; 83(5): 655–663.
43. De Minicis S and Brenner DA. NOX in liver fibrosis. *Arch Biochem Biophys* 2007; 462(2): 266–272.
44. Koek GH, Liedorp PR and Bast A. The role of oxidative stress in non-alcoholic steatohepatitis. *Clin Chim Acta* 2011; 412(15–16): 1297–1305.
45. Gough KM, Tzadu L, Kastyak MZ, et al. Theoretical and experimental considerations for interpretation of amide I bands in tissue. *Vib Spectrosc* 2010; 53(1): 71–76.
46. Zohdi V, Whelan DR, Wood BR, et al. Importance of tissue preparation methods in FTIR micro-spectroscopical analysis of biological tissues: 'traps for new users'. *PLoS One* 2015; 10(2): e0116491.